RSC Advances

PAPER

View Article Online
View Journal | View Issue

Cite this: *RSC Adv.*, 2020, **10**, 35090

Flexible electrospun PVDF–$BaTiO_3$ hybrid structure pressure sensor with enhanced efficiency

Sahar Kalani,[a] Reza Kohandani[b] and Roohollah Bagherzadeh *[acd]

Ceramic doped-polymer structures as organic and inorganic hybrid structures constitute a new area of advanced materials for flexible and stretchable sensors and actuators. Here, uniform ceramic-polymer composites of tetragonal $BaTiO_3$ and polyvinylidene fluoride (PVDF) were prepared using solution casting to improve the pressure sensitivity. By introducing Ba–TiO_3 nanoparticles to PVDF nanofibers, piezoelectricity and pressure sensitivity of hybrid nanofiber mats were significantly improved. In addition, we proposed a novel flexible and stretchable multilayered pressure sensor composed of electrospun nanocomposite fibers with high electrical sensitivity up to 6 mV N^{-1} compared to 1.88 mV N^{-1} for the pure PVDF sensors upon the application of cyclic loads at 2.5 Hz frequency and a constant load of 0.5 N. Indeed, this work provides a composition-dependent approach for the fabrication of nanostructures for pressure sensors in a wide variety of wearable devices and technologies.

Received 29th June 2020
Accepted 1st September 2020

DOI: 10.1039/d0ra05675h

rsc.li/rsc-advances

Introduction

In the past decade, very accurate nanostructured pressure sensors with different kinds of nanomaterials including nanofibers,[1] nanotubes,[2] nanowires,[3] nanoparticles,[4] *etc.* have been developed. These kinds of pressure sensors use the tuning of resistance,[3b,5] capacitance,[1c,6] piezoelectricity[3a,7] and triboelectricity[8] to measure the amount of external pressure. Polymeric piezoelectric materials are interesting candidates for sensing applications due to their flexibility, low-cost manufacturing process and low processing temperature.[9] Lead zirconate titanate (PZT) is a commonly used piezoelectric material due to its high piezoelectricity voltage.[10] However, lead-free piezoelectric materials are of more practical interest as PZT can produce harmful heavy metals when it is employed and sintered.[11] Accordingly, $BaTiO_3$ as an environmental friendly material has become an interesting candidate for energy harvesting devices.[12] Besides, $BaTiO_3$ provides better energy transfer in pressure sensors due to its higher piezoelectric strain coefficient.[13] Nevertheless, it has poor mechanical strength and breaks easily, which prevents its application in wearable materials.[14] To prevent this, it is combined with polymeric materials such as PVDF to convert it into a flexible combination for these purposes.[15]

PVDF is one of the most technically important piezoelectric polymers and is widely employed in the area of sensors, energy harvesting and health monitoring.[16] Strong piezoelectricity effect of PVDF was firstly reported by Kawai in 1969.[17] PVDF has a semi-crystalline structure which is represented by repeated monomer unites of $-CH_2-CF_2-$.[17] Considering mentioned structure for PVDF, it can be regarded polar due to electropositive hydrogen atoms and electronegative fluorine atoms in contrast to the carbon chain.[17] PVDF demonstrates four crystalline phases, determined as α, β, γ and δ.[18] Although, α-phase is the most abundant phase among the all phases, β-phase possess the most ferroelectric and piezoelectric effects.[19] PVDF as a polymorphic material can exhibit various phases depending on the processing condition.[20] Recent works on PVDF shows that an effective way to produce β-phase in PVDF is fabricating nanofiber mats using electrospinning under different preparation conditions.[20] However, resulted PVDF mats most often show a mixed of α and β-phase after electrospinning process.[21] By adding magnetic nanoparticles and additives to the PVDF solution during the electrospinning process, a PVDF electrospun nanofiber mat with a dominant β-phase can be achieved.[22] Using $BaTiO_3$ nanoparticles as an additive material, a superior piezoelectric and ferroelectric properties can be induced to PVDF nanofiber mats.[23]

There has been considerable attention on the flexible pressure sensors in the last decade due to their easy fabrication process, low cost, easy electrical signal acquisition and *etc.*[15,24] This kind of sensors made from piezoelectric sensitive materials, convert mechanical forces to electrical voltage. On the other hand, applying external forces on piezoelectric materials leads to a separation between positive and negative charges inside the material resulting a potential difference within the material.[25] Accordingly, the amount of external pressure can be determined based on the generated voltage within the material.[25] Depending

[a]*Advanced Fibrous Materials LAB, Institute for Advanced Textile Materials and Technologies (ATMT), School of Advanced Materials and Processes, Amirkabir University of Technology, Tehran, Iran. E-mail: Bagherzadeh_r@aut.ac.ir*
[b]*Department of Electrical and Computer Engineering, University of Waterloo, 200 University Avenue West, Waterloo, ON, N2L 3G1, Canada*
[c]*Institute for Frontier Materials (IFM), Deakin University, Geelong, VIC, Australia*
[d]*The School of Textiles, Donghua University (DHU), Shanghai, China*

on the application, various flexible substrate can be employed for the pressure sensors including; polyimide, polyethylene terephthalate (PET) film, polydimethylsiloxane (PDMS) film and flexible nanofiber mats.[25] In a previous study, Persano *et al.*,[1a] developed an electrospun pressure sensor based on poly(-vinylidenefluoride–trifluoroethylene) (P(VDF–TrFE)), which was able to detect pressures less than 0.1 Pa. Also, Akiyama *et al.*,[26] fabricated a piezoelectric pressure sensor using two platinum (Pt) thin films, an aluminum nitride (AlN) thin film and a PET film which can operate on room temperature in a pressure range of 0 to 8 MPa. In another study,[27] a novel pressure sensor based on nanowire/graphene heterostructure was developed with the potential application in E-skin and wearable devices. Furthermore, different type of pressure sensors based on PVDF/$BaTiO_3$ electrospun nanofibers have been produced. In order to improve the efficiency of these types of sensors various modification agents such as dopamine (DA),[28] poly(methyl methacrylate) (PMMA),[29] polystyrene (PS),[30] poly(glycidyl methacrylate) (PGMA)[31] and phosphonic acid[32] have been employed for surface modification. Also, more research has been conducted to prepare sandwich structures pressure sensors.[33]

In this paper a comprehensive study were performed to tune the sensitivity of flexible pressure sensors made of hybrid structure (electrospun PVDF/$BaTiO_3$ nanofibers). In addition, the sensitivities of different composite structures fabricated using nanofiber mats and gold sputtered surfaces were analyzed. To our best knowledge, this is the first research to compare the sensitivities of the hybrid nanofibers PVDF/$BaTiO_3$ and composite structure of gold-coated mats. Firstly, various PVDF pressure sensors with different PVDF solution concentration are produced and then their morphology were characterized using SEM images including the fiber diameter distribution and fiber uniformity. Then, the concentration that represent the most desirable resulted nanofibers morphology *i.e.* uniform and bead-free, selected for further experiments. Next, organic and inorganic hybrid structures consisting $BaTiO_3$ nanoparticles with different concentrations are incorporated into the PVDF solution and resulted nanofiber mats were then evaluated. Further, FTIR analyze is being employed to characterized the crystalline structure of nanofiber mats and a detailed analysis were performed to determine the effect of $BaTiO_3$ nanoparticles on crystallinity and piezoelectricity of the PVDF nanofibers. Then, the fabricated pressure sensors were tested using a novel homemade instrument called "PiezoTester" and the results were compared to depict the influence of $BaTiO_3$ nanoparticles on the performance of pressure sensors. Finally, novel sandwich nano-structured are made with PVDF, PVDF/$BaTiO_3$ and gold sputtered surfaces to achieve alternative flexible sensors. The produced sensors have a very high potential to be utilized in a wide range of application including wearable devices and health monitoring.

Surface morphology of pure PVDF

In order to select the best appropriate PVDF solution, electrospun nanofiber samples were produced in various concentrations of PVDF in the solvent mixture. The desirable PVDF solution, leads to obtaining a uniform bead-free nanofiber sample. Homogenized solutions were obtained by solving PVDF pellets in dimethylformamide (DMF) and acetone solvent in 6/4 ratio. Then the mixture was heated to 60 °C while stirring at 750 rpm for 3 hours. In electrospinning set up, high voltage, feed rate and tip to collector distance were set to 18 kV, 0.5 ml h^{-1} and 18 cm, respectively. Fig. 1(a–f) illustrates the surface morphology of the produced electrospun fibers with different PVDF concentrations of 19, 21, 23, 25, 27, 29 wt%, respectively. Moreover, fiber diameter distributions of the nanofiber samples are presented in Fig. 2(a–f), which provide valuable information about the properties of obtained nanofibers. Samples (a) (19 wt%) and (b) (21 wt%) are not appropriate samples because of the presence of non-uniform fibers with some large beads in between, which are recognizable in the SEM images. Also, samples (e) (27 wt%) and (f) (29 wt%) are not suitable because the distribution of fiber diameters show that the fibers diameter in both samples are mostly above the nanoscale size range (>1000 nm), which makes them undesirable for this work. However, increasing the concentration of PVDF has led to production of bead-free electrospun nanofibers in these two samples. Samples (c) (23 wt%) and (d) (25 wt%) have the most desirable conditions. Firstly, these samples seem to have uniform electrospun fibers with nanoscale size range. Secondly, increasing the concentration of the PVDF has led to production of nanofibers with lower bead formations. This is due to

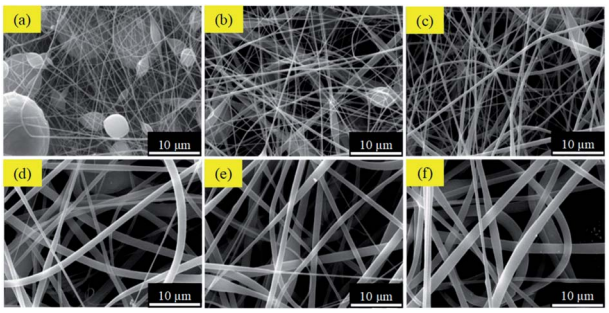

Fig. 1 (a–f) SEM images of electrospun nanofibers with different PVDF concentration of 19, 21, 23, 25, 27, 29 wt%, respectively.

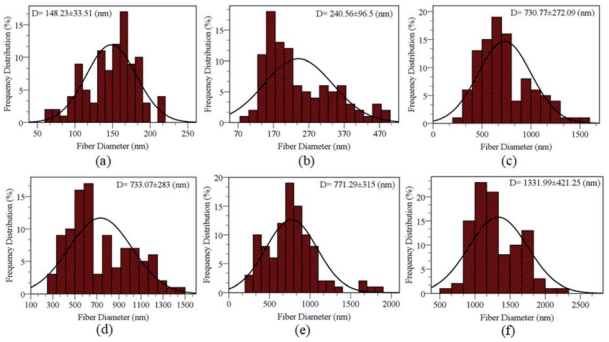

Fig. 2 (a–f) Fiber diameter distributions of electrospun nanofibers with different PVDF concentration of 19, 21, 23, 25, 27, 29 wt%, respectively.

enhancement of the solution resistance against the electrical force which is achieved because of the existence of higher amount of polymer in electrospinning jet and more interactions between the polymer chains in the solutions.[34]

Therefore, both electrospun nanofiber mats which are produced from samples (c) and (d) seem desirable for further considerations. Nevertheless, some more experiments should be carried out to introduce the best candidate.

As the final goal of present work is to implement an efficient PVDF–$BaTiO_3$ pressure sensor, it is important that produced electrospun nanofiber mat also be optimized for the maximum sensitivity. Accordingly, pressure sensitivity of the samples (c) and (d) were experimentally measured and then compared to select the best candidate. A small piece of samples (c) and (d) (12 cm^2, and thickness of 20 μm), as active layers were placed between two thin pieces of aluminum tapes, as shown in Fig. 3. Also, paper frames was utilized to keep the nanofibers mat in their original structures and decreasing the environmental noises.[38] Finally, the piezoelectric properties and sensitivity of the samples were obtained using a measurement system which were successfully used in previous studies.[35] The measurement setup consists of an impact test rig, a load cell and an oscilloscope to monitor the output response. Moreover, a preamplifier was employed to amplify the output. One remarkable feature of this PiezoTester is capability of measuring the amount of applied pressure. On the other hand, the amount of applied force and the impact head frequency can be defined and the output voltage of the piezoelectric sample can measured from the oscilloscope. Consequently, the sensitivity of the device to the applied pressure can be measured by dividing the output voltage to the applied pressure. It is worthwhile to mention that the impact head frequency has a considerable influence on the pressure sensitivity of the device. Therefore, the results in this paper are presented for different frequencies as well. More details about the experimental setup and PiezoTester can be found in ref. 35.

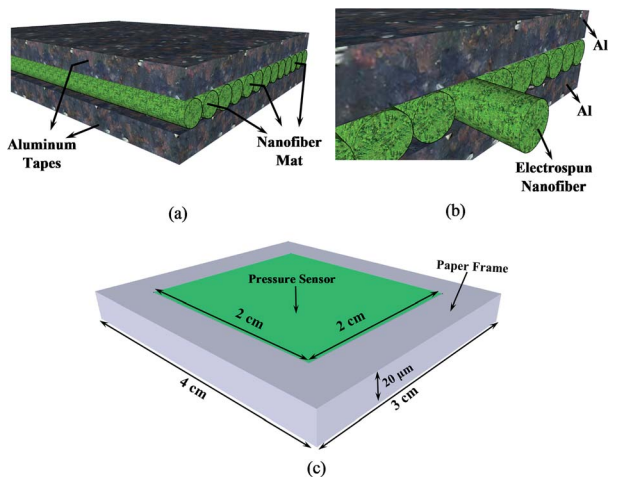

Fig. 3 (a) Schematic diagram of nanofiber mat placed between two aluminum tapes, (b) zoom-in view of the structure and (c) structure of pressure sensor and paper frame.

Fig. 4(a) and (b) demonstrate the sensitivity of the electrospun nanofiber mats of sample (c) (23 wt%) and (d) (25 wt%) as functions of force and frequency, respectively. When the frequency is constant (5 Hz) and force changes, as shown in Fig. 4(a), the sensitivity of the both samples decreases as the force increase. Also, the sensitivity of the sample (d) (25 wt%) is more than sensitivity of sample (c) (23 wt%) for all forces. When the force is constant (0.5 N) and frequency changes, as shown in Fig. 4(b), sensitivity of both samples increases. Further, one can see that for all frequencies, sample (d) has better sensitivity.

Although, it seems that sample (d) is the suitable candidate for further experiments, it is possible that the sensitivity of the samples changes by adding nanoparticles. Thus, another experiment was carried out in order to compare the sensitivity, when $BaTiO_3$ were added as nanoparticles to both samples. $BaTiO_3$ in powder form with less than 100 nm size, were used as the filler to integrate with PVDF substrate matrix. $BaTiO_3$ particles were incorporated into the polymer matrix by the blending technique. The $BaTiO_3$ powder and PVDF pellets were solved in DMF and acetone simultaneously in 6/4 ratio. The solution was stirred for about 4 hours at 60 °C in 750 rpm and sonicated for 1 hour to obtain a homogenized solution. This processing method allowed us to obtain an extraordinary uniform dispersion of the $BaTiO_3$ particles within the PVDF polymer matrix. Therefore, two different nanofiber mats were produced with PVDF with concentration of (23 wt%) and (25 wt%) mixed with $BaTiO_3$ (22 wt%) as nanoparticles. Finally, a small piece of each samples (12 cm^2, and thickness of 20 μm), were placed between two thin pieces of aluminum tapes and two pieces of paper frames and sensitivity of samples were measured using the measurement device. Fig. 4(c) and (d)

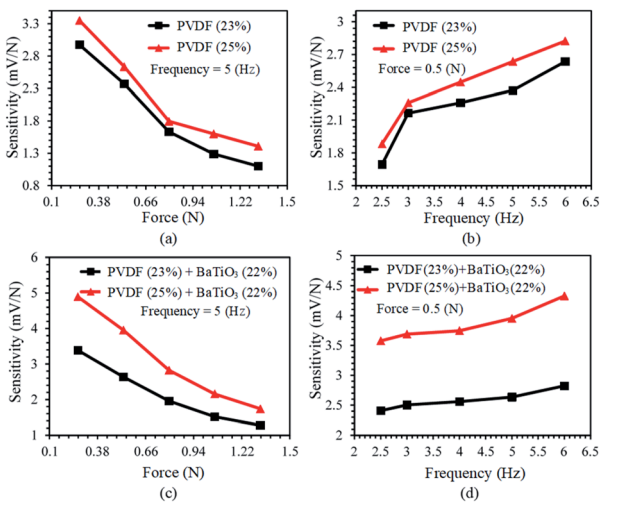

Fig. 4 (a) Sensitivity of nanofiber samples (c) and (d) when frequency is constant and force changes, (b) sensitivity of nanofiber samples (c) and (d) when force is constant and frequency changes, (c) sensitivity of produced nanofiber mats from mixture of $BaTiO_3$ (22 wt%) with samples (c) and (d), when frequency is constant and force changes, and (d) sensitivity of produced nanofiber mats from mixture of $BaTiO_3$ (22 wt%) with samples (c) and (d), when force is constant and frequency changes.

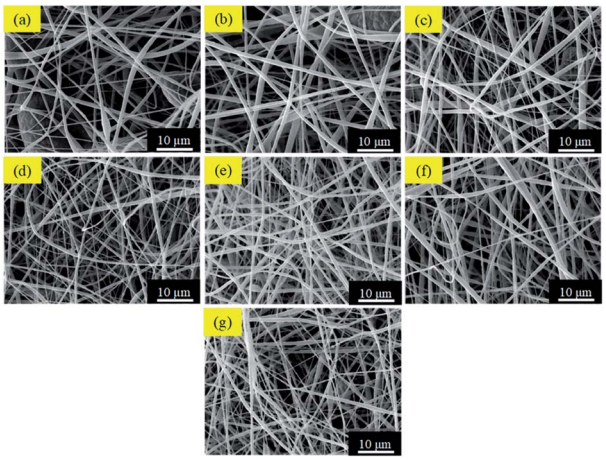

Fig. 5 (a–g) SEM images of produced electrospun nanofiber from PVDF/$BaTiO_3$ solution with PVDF concentration of 25 wt% and various $BaTiO_3$ concentrations of 6 wt%, 12 wt%, 18 wt%, 20 wt%, 22 wt%, 24 wt% and 26 wt%, respectively.

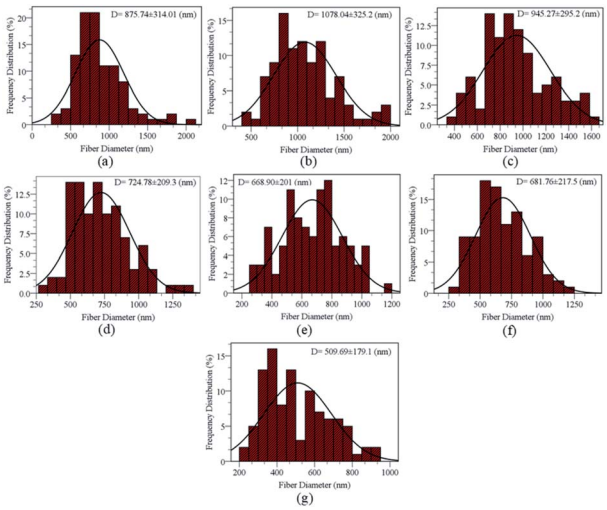

Fig. 6 (a–g) Fiber diameter distributions of electrospun nanofibers of PVDF/$BaTiO_3$ solution with PVDF concentration of 25 wt% and various $BaTiO_3$ concentrations of 6 wt%, 12 wt%, 18 wt%, 20 wt%, 22 wt%, 24 wt% and 26 wt%, respectively.

illustrate the sensitivity of the electrospun nanofibers made of samples (c) and (d) with additional $BaTiO_3$ (22 wt%), as nanoparticles. At constant frequency (5 Hz), as shown in Fig. 4(c), an enhancement in the applied force leads to reduction in sensitivity of both samples. Further, mixture of sample (d) with $BaTiO_3$ nanoparticles has higher sensitivity in compare with mixture of sample (c) with $BaTiO_3$, for all forces. At constant force (0.5), as illustrated in Fig. 4(d), sensitivity of both samples increases by enhancing the frequency. However, mixture of sample (d) with $BaTiO_3$ has better sensitivity in compare with mixture of sample (c) with $BaTiO_3$, for all frequencies.

As a result, sample (d) with 25% concentration of PVDF, has better morphology and sensitivity, in compare to other samples and it is considered for further experiments for production of PVDF/$BaTiO_3$ electrospun nanofiber mat.

Surface morphology of PVDF/$BaTiO_3$ nanofiber mat

Fig. 5 demonstrates SEM results of the electrospun PVDF/$BaTiO_3$ nanofiber mat for PVDF 25 wt% and different $BaTiO_3$ concentrations of 6, 12, 18, 20, 22, 24 and 26 wt%, respectively. Moreover, fiber diameter distributions of all samples are shown in the Fig. 6. It has been observed experimentally that increasing the concentration of $BaTiO_3$ more than 26% caused clogging at the needle tip. As a result the electrospinning process was stopped. One can see from Fig. 5 and 6 that introducing nanoparticles of $BaTiO_3$ to the PVDF nanofiber, decreased the nanofiber diameter and caused lower beads formation. This improvement is because of the larger elongation of PVDF/$BaTiO_3$ nanofibers which comes from the fact that polymer solution of PVDF/$BaTiO_3$ creates higher charge density in the electrospinning jet in compare to pure PVDF polymer solution.[36] However, still some beads formations can be seen in $BaTiO_3$ concentration of 6 wt%, as shown in Fig. 5(a). Although SEM image of produced nanofiber with $BaTiO_3$ concentration of 12 wt% has shown some beads formation (Fig. 5(b)), it has lower beads in compare to concentration of 6 wt%. Fig. 5(c) illustrates fiber morphology of the electrospun PVDF/$BaTiO_3$ nanofiber with $BaTiO_3$ concentration of 18 wt%. One can easily conclude from Fig. 5(c) that produced nanofiber has much lower beads in compare to previous samples. Nevertheless, it is obvious from Fig. 6(c), which shows the fiber diameter distributions of 18 wt% sample, nanofibers are not uniformly distributed in this sample. SEM images and fiber diameter distributions of electrospun nanofibers with $BaTiO_3$ concentration of 20 wt%, 22 wt%, 24 wt% and 26 wt% are shown in Fig. 5(d–g) and 6(d–g), respectively. Based on the SEM images and diameter distributions curves, theses nanofiber samples are bead-free and uniformly distributed. As a result, increasing the concentration of $BaTiO_3$ also has improved the nanofiber morphology.

Fourier transform infrared spectroscopy (FTIR) analysis

FTIR test has been employed to analyze the structure of produced nanofiber mats and to confirm their crystallinity. FTIR results of electrospun nanofiber mats, produced from PVDF 25 wt% and PVDF/$BaTiO_3$ with various concentrations of $BaTiO_3$ are shown in Fig. 7. The IR spectra of PVDF and PVDF/$BaTiO_3$ nanofiber mats are showing peaks at 613, 762, 841, 879, 975, 1070, 1187, 1280 and 1402 cm^{-1}. As depicted in the Fig. 7, the peaks at 613, 762 and 975 cm^{-1} are for α phase of the PVDF.[37] Further, the peaks at 841 and 1280 cm^{-1} are attributed to β phase of PVDF.[37] The peaks at 613 and 762 cm^{-1} are because of CF_2 and skeletal bending of C (F)–C (H)–C (F) of α phase of the PVDF, while the peak at 975 cm^{-1} is due to CH_2 bending mode of α phase.[37] One can easily conclude that the produced PVDF and PVDF/$BaTiO_3$ nanofiber mats, present a mixed structure of α and β phases. Further, because of introducing $BaTiO_3$ nanoparticles to the PVDF nanofiber mat, intensities of the absorption peaks of α phase have been attenuated.

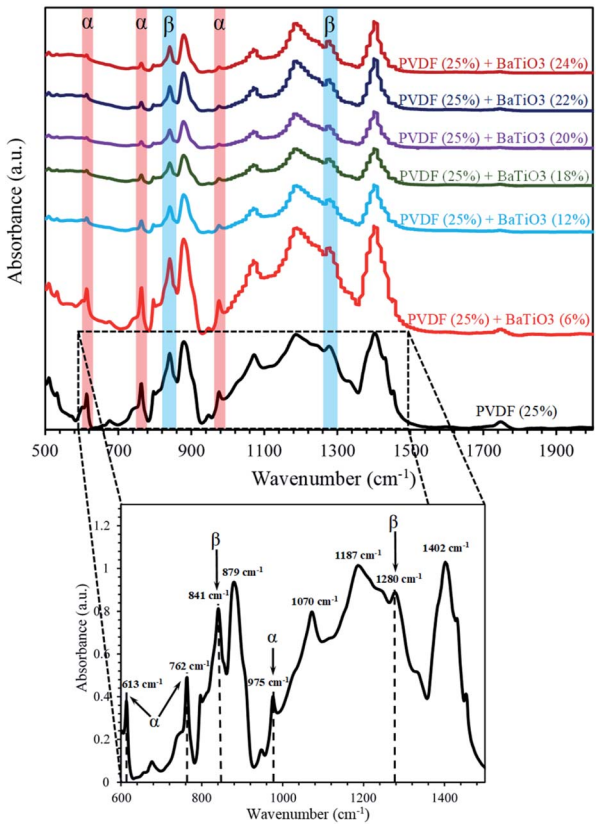

Fig. 7 FTIR results of electrospun nanofiber mats made of PVDF and PVDF/$BaTiO_3$ with various concentrations of $BaTiO_3$. A magnified spectra for pure PVDF is shown with more details.

This means that formation of β phase has been promote due to crystallization of PVDF in PVDF/$BaTiO_3$ nanofiber during the electrospinning. Fig. 8(a) shows FTIR results of PVDF/$BaTiO_3$ electrospun nanofiber as functions of wavenumber and concentrations of $BaTiO_3$. It is crystal clear from this figure that

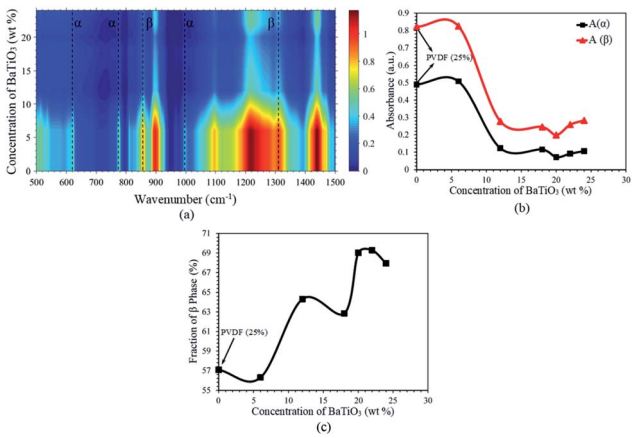

Fig. 8 (a) FTIR spectra of the PVDF/$BaTiO_3$ electrospun nanofiber as functions of wavenumber and concentration of $BaTiO_3$ nanoparticles, (b) variations of absorbance peaks of α and β phases as a function of $BaTiO_3$ concentrations, and (c) variations of fraction of β as a function of $BaTiO_3$ concentrations. Zero concentration stands for PVDF 25 wt% in all plots.

absorption peaks of α phases are diminished in intensities as a result of increasing the $BaTiO_3$ concentration. Quantity of fraction of β phase in electrospun mat, can be calculated using below equation:[38]

$$F(\beta) = \frac{A_\beta}{(1.26A_\alpha + A_\beta)} \quad (1)$$

where A_α and A_β stand for absorbances of α and β phases, respectively. Fraction of β phase is calculated using the characteristic absorption bands of α and β phases at 762 cm^{-1} and 841 cm^{-1}, respectively.[37]

It is assumed that these absorbances follow the Beer–Lambert law.[37] Fig. 8(b) illustrates the variations of A_α and A_β as a function of $BaTiO_3$ concentration where A_α and A_β are calculated from absorption intensities at 762 cm^{-1} and 841 cm^{-1}, respectively.[37] Zero concentration of $BaTiO_3$ means that the absorbances are calculated for PVDF 25 wt% electrospun nanofiber, as shown in the Fig. 8(b). It is obvious from Fig. 8(b) that absorption intensities of both α and β phases are decreased by increasing the concentration of $BaTiO_3$ nanoparticles. Further, fraction of β is calculated and shown for various concentration of $BaTiO_3$. Concentration of zero stands for PVDF 25 wt% electrospun nanofiber. It is clear that fraction of β is properly improved from 50% to 70%, after increasing the concentration of $BaTiO_3$.

Pressure sensitivity of PVDF/$BaTiO_3$ electrospun nanofiber mats

To evaluate the performance of the produced sensors each sample were tested separately with the PiezoTester. Samples were placed between two aluminum tapes and then a small piece of each sample with 12 cm^2 to 20 μm thickness were placed between within the paper frames (Fig. 3(c)). The pressure sensors were subjected to the periodic forces using PiezoTester and the output voltage as a function of force and frequency were achieved for different samples. The produced samples showed appropriate stability against high amount of applied forces in our experiments. Also, each piezoelectricity test was repeated five times in order to achieve valid results. Fig. 9 shows the sensitivity result of PVDF/$BaTiO_3$ pressure sensors as a function of frequency and force. As Fig. 9(a) illustrates, a constant frequency of 5 Hz were assigned to the PiezoTester and the sensitivity of the samples were measured under different forces. After adding $BaTiO_3$ nanoparticles to the PVDF samples the sensitivity of the sensors increases in all forces. This is due to higher capability of $BaTiO_3$ nanoparticles in transferring energy and thus improving the fraction of β-phase which enhances the piezoelectricity and pressures sensitivity of PVDF/$BaTiO_3$ samples. A 3 dimensional curve of sensitivity as a function of force and $BaTiO_3$ percentage is presented in Fig. 9(b). As can be seen, increasing the $BaTiO_3$ percentage has improved the sensitivity of the samples. Also, sensitivity is higher when applied forces decrease. The highest sensitivity which is achieved in this configuration is 5.6 mV N^{-1}. Fig. 9(c) and (d) show the sensitivity of the samples in a constant force of 0.5 N and different frequencies. Again, as the percentage of $BaTiO_3$

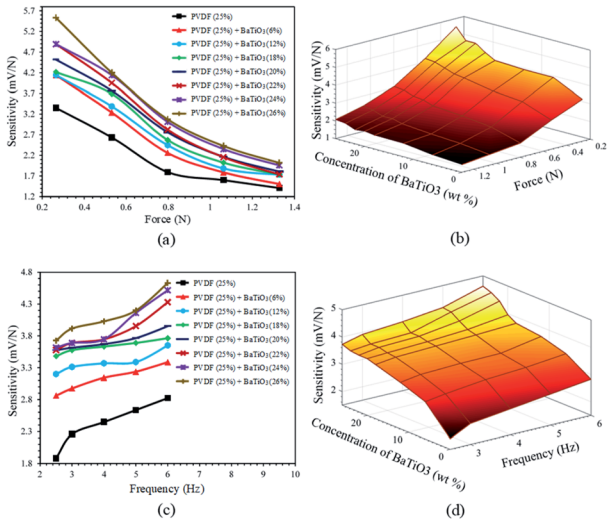

Fig. 9 (a) Sensitivity of produced pressure sensors as a functional of applied forces at constant frequency of 5 Hz, (b) sensitivity at constant frequency as a function of force and concentration of $BaTiO_3$, (c) sensitivity of produced pressure sensors as a functional of frequency at constant force of 0.5 N and (d) sensitivity at constant force as a function of frequency and concentration of $BaTiO_3$.

increases the sensitivity improves. In addition, by increasing frequency the sensitivity of old samples increases as well. The highest sensitivity which is resulted in this configuration is 4.7 mV N^{-1}.

Pressure sensitivity of (PVDF)–(PVDF/$BaTiO_3$)–(PVDF) electrospun nanocomposite

In order to improve the efficiency of the fabricated PVDF/$BaTiO_3$ pressure sensor, nanocomposite structures were also developed and tested using the most efficient PVDF and PVDF/$BaTiO_3$ nanofiber mats. As mentioned before, PVDF 25 wt% solution was the desirable candidate for producing PVDF nanofibers and PVDF/$BaTiO_3$ solution with 26 wt% of $BaTiO_3$ nanoparticles demonstrated the best pressure sensitivity. Fig. 10 shows three different configurations of electrospun nanocomposite among the others. In the first configuration shown in Fig. 10(a), a three layer nanocomposite was made in a way that a PVDF/$BaTiO_3$ mat were sandwiched between two PVDF mats by continuously spraying the solutions using electrospinning device. In this approach, firstly the PVDF solution (25 wt%) were sprayed, and then the PVDF/$BaTiO_3$ solution (25 wt% and 26 wt% of $BaTiO_3$ nanoparticle) was sprayed immediately on top of it and then a PVDF solution (25 wt%) was continuously sprayed to produce a three layer electrospun nanocomposite. Eventually, the nanocomposite was placed between aluminum tapes and paper frames (same as Fig. 3) to be tested. In the second configuration, as shown in Fig. 10(b), a PVDF/$BaTiO_3$ mat were placed between two PVDF nanofiber mats. The only different between this configuration and the previous configuration is that nanofiber mats were sprayed separately, *i.e.* each nanofiber mat were produced and removed from the collector drum and then the other nanofiber mat were sprayed. Accordingly, the

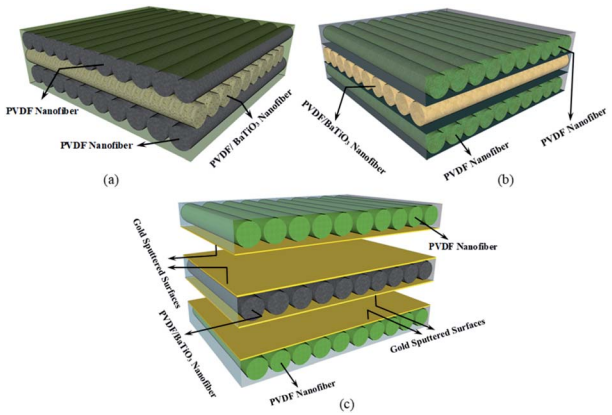

Fig. 10 (PVDF)–(PVDF/$BaTiO_3$)–(PVDF) three layer electrospun nanocomposite, (a) continuously sprayed, (b) separately sprayed and (c) separately sprayed with gold sputtered surfaces.

configuration of Fig. 10(b) was created by placing each electrospun mats manually on top of each other. Furthermore, for the measurement purpose the nanofibers were placed between the aluminum tapes and paper frames. In the last configuration as shown in Fig. 10(c), the electrospun nanocomposite was assembled using gold sputtered nanofiber mats. Both sides of PVDF/$BaTiO_3$ mats and one side of PVDF mats were gold sputtered and the nanofibers mats were assembled in a way to configure the nanocomposite of Fig. 10(c). Here gold sputtered surfaces would act as electrodes to transfer the electrical charges with more efficiency. Finally, the nanocomposites were placed between aluminum tapes and paper frames to be tested.

Fig. 11 illustrates the sensitivity results for the electrospun nanocomposites with three different configurations. In the constant frequency of 5 Hz, as shown in Fig. 11(a), at lower applied forces, the separately sprayed configuration has the best sensitivity. However, as the applied force increases the continuously sprayed configuration provides a higher sensitivity in compare with other configurations that makes it suitable for high pressures applications. Furthermore, the separately sprayed configuration shows higher sensitivity in lower applied forces, which makes it more applicable for low-pressure application. The sensitivity of gold sputtered configuration does not change a lot with increasing the amount of applied forces that can be regarded as an appropriate feature for some specific

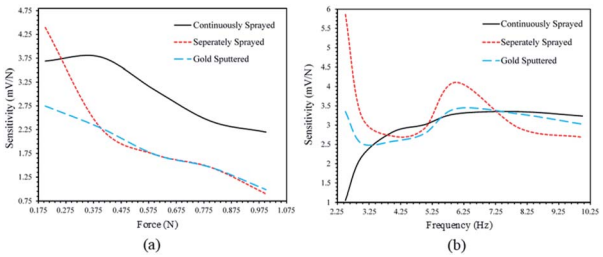

Fig. 11 Pressure sensitivity of three different electrospun nanocomposites as a function of (a) applied force in a constant frequency of 5 Hz, and (b) frequency in a constant applied force of 0.5 N.

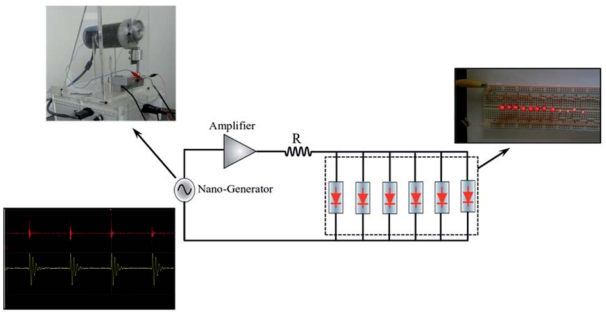

Fig. 12 The schematic diagram of the electrical circuit and some real picture of the measurement set up including; PiezoTester, voltage output, and LED.

applications. Moreover, in higher applied forces, separately sprayed configuration and gold sputtered ones almost show same trend. In constant force of 0.5 N, based on Fig. 11(b), at lower frequencies a high sensitivity of 6 mV N^{-1} is achieved by separately sprayed configuration. As a result, separately sprayed nanocomposite indicates the best performance for lower frequencies and lower pressure applications. This might be attributed to the enhancement of bulk porosity of the sample as, it consists of separate layers being placed on each other. An increment in bulk porosity leads to reduction of relative permittivity and enhancement in deformability of nanofibers which result in increasing the output of the sample.[39] The gold sputtered configuration almost shows a frequency independent performance as the sensitivity stays the same in different frequencies. The continuously sprayed nanocomposite provides a weak sensitivity in lower frequencies. All three configurations almost have the same sensitivity in higher trends.

The achieved sensitivity here can be compared with results in ref. 35 in which a PVDF/ZnO pressure sensor has been tested with the same PiezoTester. The highest sensitivity reported by ref. 35 is 2.18 mV N^{-1} which is lower than our best result (6 mV N^{-1}).

Energy harvesting capability of the produced electrospun nanofiber mats were also addressed by connecting the amplified output of the sample to an electrical circuit. The sample could successfully turn on a couple of light emitting diodes (LED). The schematic diagram of the electrical circuit and some real picture of the measurement set up are shown in Fig. 12.

Conclusions

A PVDF/$BaTiO_3$ piezoelectric pressure sensor has been developed *via* electrospinning method. The optimized concentration of the PVDF has been selected to be blended with the $BaTiO_3$ nanoparticles to produce efficient pressure sensors. Then, electrospun nanocomposites were fabricated using optimized nanofiber mats for better functionality. Introducing $BaTiO_3$ nanoparticles to the PVDF nanofibers leads to a bead-free uniform morphology with smaller nanofiber diameter. Further, the fraction of β-phase in PVDF crystal has been extensively improved by adding $BaTiO_3$ nanoparticles. Consequently, a higher-pressure sensitivity has been observed in the PVDF–$BaTiO_3$ mat as a result of added nanoparticles. In addition, increasing the concentration of $BaTiO_3$ provides higher sensitivity and a sensitivity of 6 mV N^{-1} has been achieved for a blended electrospun mat with 26 wt% $BaTiO_3$ concentration. Finally, it was shown that the proposed electrospun nanocomposites provide different functionality in various forces and frequencies, which makes them suitable for different potential applications.

Conflicts of interest

There are no conflicts to declare.

Acknowledgements

The support provided by the Advanced Fibrous Materials LAB (http://ffm.aut.ac.ir), ATMT Institute, Amirkabir University of Technology (Tehran Polytechnic), Department of Electrical and Computer Engineering, University of Waterloo, and INSF (Grant No. 97016813) are highly appreciated.

References

1 (*a*) L. Persano, C. Dagdeviren, Y. Su, Y. Zhang, S. Girardo, D. Pisignano, Y. Huang and J. A. Rogers, High performance piezoelectric devices based on aligned arrays of nanofibers of poly(vinylidenefluoride-*co*-trifluoroethylene), *Nat. Commun.*, 2013, **4**(1), 1633; (*b*) H. Lee, J. Lee, B. Seong, H. S. Jang and D. Byun, Strain Sensors: Printing Conductive Micro-Web Structures *via* Capillary Transport of Elastomeric Ink for Highly Stretchable Strain Sensors, *Adv. Mater. Technol.*, 2018, **3**(2), 1870006; (*c*) J. Lee, H. Kwon, J. Seo, S. Shin, J. H. Koo, C. Pang, S. Son, J. H. Kim, Y. H. Jang and D. E. Kim, Conductive fiber-based ultrasensitive textile pressure sensor for wearable electronics, *Adv. Mater.*, 2015, **27**(15), 2433–2439.

2 (*a*) M. Jian, K. Xia, Q. Wang, Z. Yin, H. Wang, C. Wang, H. Xie, M. Zhang and Y. Zhang, Flexible and highly sensitive pressure sensors based on bionic hierarchical structures, *Adv. Funct. Mater.*, 2017, **27**(9), 1606066; (*b*) L. Nela, J. Tang, Q. Cao, G. Tulevski and S.-J. Han, Large-area high-performance flexible pressure sensor with carbon nanotube active matrix for electronic skin, *Nano Lett.*, 2018, **18**(3), 2054–2059.

3 (*a*) R. Bao, C. Wang, L. Dong, R. Yu, K. Zhao, Z. L. Wang and C. Pan, Flexible and controllable piezo-phototronic pressure mapping sensor matrix by ZnO NW/p-polymer LED array, *Adv. Funct. Mater.*, 2015, **25**(19), 2884–2891; (*b*) S. Gong, W. Schwalb, Y. Wang, Y. Chen, Y. Tang, J. Si, B. Shirinzadeh and W. Cheng, A wearable and highly sensitive pressure sensor with ultrathin gold nanowires, *Nat. Commun.*, 2014, **5**(1), 1–8.

4 (*a*) X. Wang, H. Zhang, R. Yu, L. Dong, D. Peng, A. Zhang, Y. Zhang, H. Liu, C. Pan and Z. L. Wang, Dynamic pressure mapping of personalized handwriting by a flexible sensor matrix based on the mechanoluminescence process, *Adv.*

Mater., 2015, **27**(14), 2324–2331; (*b*) D. Lee, H. Lee, Y. Jeong, Y. Ahn, G. Nam and Y. Lee, Highly Sensitive, Transparent, and Durable Pressure Sensors Based on Sea-Urchin Shaped Metal Nanoparticles, *Adv. Mater.*, 2016, **28**(42), 9364–9369.

5 H. Chen, Z. Su, Y. Song, X. Cheng, X. Chen, B. Meng, Z. Song, D. Chen and H. Zhang, Omnidirectional bending and pressure sensor based on stretchable CNT-PU sponge, *Adv. Funct. Mater.*, 2017, **27**(3), 1604434.

6 J. Wang, J. Jiu, M. Nogi, T. Sugahara, S. Nagao, H. Koga, P. He and K. Suganuma, A highly sensitive and flexible pressure sensor with electrodes and elastomeric interlayer containing silver nanowires, *Nanoscale*, 2015, **7**(7), 2926–2932.

7 B. Wang, C. Liu, Y. Xiao, J. Zhong, W. Li, Y. Cheng, B. Hu, L. Huang and J. Zhou, Ultrasensitive cellular fluorocarbon piezoelectret pressure sensor for self-powered human physiological monitoring, *Nano Energy*, 2017, **32**, 42–49.

8 (*a*) T. Li, J. Zou, F. Xing, M. Zhang, X. Cao, N. Wang and Z. L. Wang, From dual-mode triboelectric nanogenerator to smart tactile sensor: a multiplexing design, *ACS Nano*, 2017, **11**(4), 3950–3956; (*b*) J. Zou, M. Zhang, J. Huang, J. Bian, Y. Jie, M. Willander, X. Cao, N. Wang and Z. L. Wang, Coupled supercapacitor and triboelectric nanogenerator boost biomimetic pressure sensor, *Adv. Energy Mater.*, 2018, **8**(10), 1702671.

9 Y. Bar-Cohen and Q. Zhang, Electroactive polymer actuators and sensors, *MRS Bull.*, 2008, **33**(3), 173–181.

10 F. R. Fan, W. Tang and Z. L. Wang, Flexible nanogenerators for energy harvesting and self-powered electronics, *Adv. Mater.*, 2016, **28**(22), 4283–4305.

11 Y. Saito, H. Takao, T. Tani, T. Nonoyama, K. Takatori, T. Homma, T. Nagaya and M. Nakamura, Lead-free piezoceramics, *Nature*, 2004, **432**(7013), 84–87.

12 (*a*) A. D. Hussein, R. S. Sabry, O. A. A. Dakhil and R. Bagherzadeh, Effect of Adding $BaTiO_3$ to PVDF as Nano Generator, *J. Phys.: Conf. Ser.*, 2019, 022012; (*b*) Z.-M. Dang, J.-K. Yuan, J.-W. Zha, T. Zhou, S.-T. Li and G.-H. Hu, Fundamentals, processes and applications of high-permittivity polymer–matrix composites, *Prog. Mater. Sci.*, 2012, **57**(4), 660–723; (*c*) L. Wang, M. R. Cho, Y. J. Shin, J. R. Kim, S. Das, J.-G. Yoon, J.-S. Chung and T. W. Noh, Overcoming the fundamental barrier thickness limits of ferroelectric tunnel junctions through $BaTiO_3$/$SrTiO_3$ composite barriers, *Nano Lett.*, 2016, **16**(6), 3911–3918.

13 (*a*) A. Koka and H. A. Sodano, A low-frequency energy harvester from ultralong, vertically aligned $BaTiO_3$ nanowire arrays, *Adv. Energy Mater.*, 2014, **4**(11), 1301660; (*b*) J. Briscoe and S. Dunn, Piezoelectric nanogenerators – a review of nanostructured piezoelectric energy harvesters, *Nano Energy*, 2015, **14**, 15–29.

14 H. Zhang, L. Zhang, Q. Jia, C. Shi and J. Yang, Preparation of porous nylon 6 fiber *via* electrospinning, *Polym. Eng. Sci.*, 2015, **55**(5), 1133–1141.

15 K. Shi, B. Sun, X. Huang and P. Jiang, Synergistic effect of graphene nanosheet and $BaTiO_3$ nanoparticles on performance enhancement of electrospun PVDF nanofiber mat for flexible piezoelectric nanogenerators, *Nano Energy*, 2018, **52**, 153–162.

16 H. Wu, Y. Huang, F. Xu, Y. Duan and Z. Yin, Energy harvesters for wearable and stretchable electronics: from flexibility to stretchability, *Adv. Mater.*, 2016, **28**(45), 9881–9919.

17 H. Kawai, The piezoelectricity of poly(vinylidene fluoride), *Jpn. J. Appl. Phys.*, 1969, **8**(7), 975.

18 H. S. Nalwa, *Ferroelectric polymers: chemistry: physics, and applications*, CRC Press, 1995.

19 M. Li, H. J. Wondergem, M.-J. Spijkman, K. Asadi, I. Katsouras, P. W. Blom and D. M. De Leeuw, Revisiting the δ-phase of poly(vinylidene fluoride) for solution-processed ferroelectric thin films, *Nat. Mater.*, 2013, **12**(5), 433–438.

20 J. Zheng, A. He, J. Li and C. C. Han, Polymorphism control of poly(vinylidene fluoride) through electrospinning, *Macromol. Rapid Commun.*, 2007, **28**(22), 2159–2162.

21 J. Andrew and D. Clarke, Effect of electrospinning on the ferroelectric phase content of polyvinylidene difluoride fibers, *Langmuir*, 2008, **24**(3), 670–672.

22 J. Andrew and D. Clarke, Enhanced ferroelectric phase content of polyvinylidene difluoride fibers with the addition of magnetic nanoparticles, *Langmuir*, 2008, **24**(16), 8435–8438.

23 (*a*) Z.-M. Dang, D. Xie and C.-Y. Shi, Theoretical prediction and experimental study of dielectric properties in poly(vinylidene fluoride) matrix composites with micronanosize $BaTiO_3$ filler, *Appl. Phys. Lett.*, 2007, **91**(22), 222902; (*b*) C. Chanmal and J. Jog, Dielectric relaxations in PVDF/$BaTiO_3$ nanocomposites, *eXPRESS Polym. Lett.*, 2008, **2**(4), 294–301.

24 (*a*) C. Bowen, H. Kim, P. Weaver and S. Dunn, Piezoelectric and ferroelectric materials and structures for energy harvesting applications, *Energy Environ. Sci.*, 2014, **7**(1), 25–44; (*b*) W. Wu and Z. L. Wang, Piezotronics and piezo-phototronics for adaptive electronics and optoelectronics, *Nat. Rev. Mater.*, 2016, **1**(7), 1–17; (*c*) S. Liu, L. Wang, Z. Wang, Y. Cai, X. Feng, Y. Qin and Z. L. Wang, Double-channel piezotronic transistors for highly sensitive pressure sensing, *ACS Nano*, 2018, **12**(2), 1732–1738.

25 F. Xu, X. Li, Y. Shi, L. Li, W. Wang, L. He and R. Liu, Recent developments for flexible pressure sensors: a review, *Micromachines*, 2018, **9**(11), 580.

26 M. Akiyama, Y. Morofuji, T. Kamohara, K. Nishikubo, M. Tsubai, O. Fukuda and N. Ueno, Flexible piezoelectric pressure sensors using oriented aluminum nitride thin films prepared on polyethylene terephthalate films, *J. Appl. Phys.*, 2006, **100**(11), 114318.

27 Z. Chen, Z. Wang, X. Li, Y. Lin, N. Luo, M. Long, N. Zhao and J.-B. Xu, Flexible piezoelectric-induced pressure sensors for static measurements based on nanowires/graphene heterostructures, *ACS Nano*, 2017, **11**(5), 4507–4513.

28 Z. Wang, T. Wang, C. Wang, Y. Xiao, P. Jing, Y. Cui and Y. Pu, Poly(vinylidene fluoride) flexible nanocomposite films with dopamine-coated giant dielectric ceramic nanopowders, $Ba(Fe_{0.5}Ta_{0.5})O_3$, for high energy-storage density at low

electric field, *ACS Appl. Mater. Interfaces*, 2017, **9**(34), 29130–29139.

29 K. Yang, X. Huang, M. Zhu, L. Xie, T. Tanaka and P. Jiang, Combining RAFT polymerization and thiol–ene click reaction for core–shell structured polymer@$BaTiO_3$ nanodielectrics with high dielectric constant, low dielectric loss, and high energy storage capability, *ACS Appl. Mater. Interfaces*, 2014, **6**(3), 1812–1822.

30 X. Huang and P. Jiang, Core–shell structured high-k polymer nanocomposites for energy storage and dielectric applications, *Adv. Mater.*, 2015, **27**(3), 546–554.

31 M. Ejaz, V. S. Puli, R. Elupula, S. Adireddy, B. C. Riggs, D. B. Chrisey and S. M. Grayson, Core–shell structured poly(glycidyl methacrylate)/$BaTiO_3$ nanocomposites prepared by surface-initiated atom transfer radical polymerization: A novel material for high energy density dielectric storage, *J. Polym. Sci., Part A: Polym. Chem.*, 2015, **53**(6), 719–728.

32 P. Kim, N. M. Doss, J. P. Tillotson, P. J. Hotchkiss, M.-J. Pan, S. R. Marder, J. Li, J. P. Calame and J. W. Perry, High energy density nanocomposites based on surface-modified $BaTiO_3$ and a ferroelectric polymer, *ACS Nano*, 2009, **3**(9), 2581–2592.

33 (*a*) K. Saetia, J. M. Schnorr, M. M. Mannarino, S. Y. Kim, G. C. Rutledge, T. M. Swager and P. T. Hammond, Spray-Layer-by-Layer Carbon Nanotube/Electrospun Fiber Electrodes for Flexible Chemiresistive Sensor Applications, *Adv. Funct. Mater.*, 2014, **24**(4), 492–502; (*b*) H. Park, Y. R. Jeong, J. Yun, S. Y. Hong, S. Jin, S.-J. Lee, G. Zi and J. S. Ha, Stretchable array of highly sensitive pressure sensors consisting of polyaniline nanofibers and Au-coated polydimethylsiloxane micropillars, *ACS Nano*, 2015, **9**(10), 9974–9985.

34 A. S. Motamedi, H. Mirzadeh, F. Hajiesmaeilbaigi, S. Bagheri-Khoulenjani and M. Shokrgozar, Effect of electrospinning parameters on morphological properties of PVDF nanofibrous scaffolds, *Prog. Biomater.*, 2017, **6**(3), 113–123.

35 M. S. Sorayani Bafqi, A.-H. Sadeghi, M. Latifi and R. Bagherzadeh, Design and fabrication of a piezoelectric out-put evaluation system for sensitivity measurements of fibrous sensors and actuators, *J. Ind. Text.*, 2019, 1528083719867443.

36 E. Ghafari, X. Jiang and N. Lu, Surface morphology and beta-phase formation of single polyvinylidene fluoride (PVDF) composite nanofibers, *Adv. Compos. Hybrid Mater.*, 2018, **1**(2), 332–340.

37 C. V. Chanmal and J. P. Jog, Electrospun PVDF/$BaTiO_3$ nanocomposites: polymorphism and thermal emissivity studies, *Int. J. Plast. Technol.*, 2011, **15**(1), 1.

38 M. S. S. Bafqi, R. Bagherzadeh and M. Latifi, Fabrication of composite PVDF–ZnO nanofiber mats by electrospinning for energy scavenging application with enhanced efficiency, *J. Polym. Res.*, 2015, **22**(7), 130.

39 M. M. Abdolhasani, M. Naebe, M. H. Amiri, K. Shirvanimoghaddam, S. Anwar, J. J. Michels and K. Asadi, Hierarchically Structured Porous Piezoelectric Polymer Nanofibers for Energy Harvesting, *Adv. Sci.*, 2020, 2000517.

